ADVANCED MATERIALS
www.advmat.de

Esterase-Activated Charge-Reversal Polymer for Fibroblast-Exempt Cancer Gene Therapy

*Nasha Qiu, Xiangrui Liu, Yin Zhong, Zhuxian Zhou, Ying Piao, Lei Miao, Qianzhi Zhang, Jianbin Tang, Leaf Huang, and Youqing Shen**

Cationic polymers have been extensively explored as nonviral gene vectors owing to their nonimmonogenity and safe nature.[1] Recently, the combinatorial library approach[2] has identified many structures with enhanced capabilities for siRNA delivery[3] and codelivery.[4,5] As the current transfection efficiencies are still much lower than viral vectors,[6] prevailing efforts on nonviral DNA vectors are still focused on how to increase DNA transcription efficiency including optimizing molecular structures[7] and nanostructures[8] as well as studying mechanism.[9] Alternatively, how to exploit the characters of nonviral vectors to maximize their therapeutic advantages to merit clinical translation would be an equally important direction.

It has recently been shown that damaging fibroblasts in cancer treatment induces their hyperactivation to secrete WNT16B,[10] a signal known to strongly promote tumor cell survival and metastasis[10a], which is the main cause of quick tumor relapse and poor prognosis of chemotherapy. Thus, a therapy benign to fibroblasts may not cause their hyperactivation and lead to better prognosis. In cationic polymer-mediated gene delivery, it is known that intracellular dissociation of polymer/DNA complexes (polyplexes) to release DNA is the prerequisite for its effective transfection and translation.[11] We thus hypothesize that polyplexes with a cancer suicide gene that efficiently dissociate in cancer cells but hardly dissociate in tumor fibroblasts would realize cancer gene therapy capable of selectively killing tumor cells but avoiding fibroblast hyperactivation.

Along this line, here we show such an example of cancer-cell-selective and fibroblast-exempt polyplexes for potent cancer gene therapy using an esterase-responsive polymer (ERP) as a gene carrier made from quaternary amines carrying *N*-propionic 4-acetoxybenzyl ester substituents (**Figure 1**). The 4-acetoxybenzyl ester group can undergo a quick intracellular esterase-catalyzed hydrolysis, which subsequently triggers the polymer's charge-reversal from cationic to zwitterionic (Figure 1a). Taking advantage of the high cytosolic esterase activity in HeLa cancer cells but low level in fibroblasts, the ERP/DNA polyplexes taken up by cancer cells quickly dissociate and release the DNA due to the charge conversion, while polyplexes taken up into fibroblasts hardly dissociate due to the unchanged cationic nature of ERP, giving efficient gene expression in cancer cells but not in fibroblasts. Accordingly, a cancer suicide gene, the tumor necrosis factor related apoptosis-inducing ligand gene (pTRAIL), delivered by the system effectively induces apoptosis of cancer cells due to high TRAIL expression but does little harm to fibroblasts and thereby does not stimulate them to express WNT16B. Thus, the tumor-cell-selective gene therapy exerts very potent anticancer activity compared to chemotherapy, which causes indiscriminate killing and thus hyperactivation of fibroblasts.

Alkyl esters are generally very stable and hydrolyze very slowly, even in the presence of enzymes,[12] while phenolic acetate was reported readily hydrolyzable by esterase.[13] Thus, a 4-acetoxybenzyl ester was used as a trigger for esterase-catalyzed charge-reversal (Figure 1). The ERP polymer was synthesized from 10 kDa polyethylenimine (PEI). PEI was first reacted with p-acetoxybenzyl acrylate and quaternized. A molecular weight of 10 kDa PEI was used to keep the molecular weight of the resulting water-soluble zwitterionic polymer still below the renal clearance threshold (≈30 kDa[14]). The control polymers, i.e., quaternized PEI reacted with benzyl acrylate (QPEI-BP) and methylated quaternized PEI (QPEI-M) were synthesized and characterized similarly (Scheme S1, Supporting Information).

The esterase-catalyzed hydrolysis of the phenolic acetate moieties was tracked by monitoring the release of 4-hydroxybenzyl alcohol (HBA) by HPLC (Figure S1, Supporting Information). In the presence of esterase at 100 U mL^{-1}, HBA was already detected in 10 min and all esters were completely hydrolyzed within an hour. Simultaneously, the zeta-potential of ERP quickly changed from +10 mV to −15 mV (**Figure 2**a). This is apparently much faster than the hydrolysis of alkyl[12b,15] or benzyl[16] esters and confirms the report that esterase could selectively hydrolyze phenolic acetate over alkyl acetates.[13]

Cationic ERP effectively complexed plasmid DNA and formed relatively uniform particles (polyplexes) of 80 nm at N/P ratios greater than 10 (Figure 2b,c). The zeta-potentials of ERP polyplexes were +15 mV, much lower than those of PEI polyplexes. The ERP polyplexes were stable in medium, as evidenced by gel electrophoresis, but once treated with esterase, the polyplexes fell apart and quickly released free DNA (Figure S2A, Supporting Information).

The transfection ability of ERP polyplexes was evaluated and compared with PEI polyplexes in several cell lines

N. Qiu, Prof. X. Liu, Y. Zhong, Prof. Z. Zhou, Y. Piao, Q. Zhang, Prof. J. Tang, Prof. Y. Shen
Center for Bionanoengineering and Key Laboratory of Biomass Chemical Engineering of Ministry of Education
College of Chemical and Biological Engineering
Zhejiang University
Hangzhou 310027, China
E-mail: shenyq@zju.edu.cn
Dr. L. Miao, Prof. L. Huang
Eshelman School of Pharmacy
University of North Carolina at Chapel Hill
Chapel Hill, NC 27599, USA

DOI: 10.1002/adma.201603095

ADVANCED MATERIALS
www.advmat.de

Materials Views
www.MaterialsViews.com

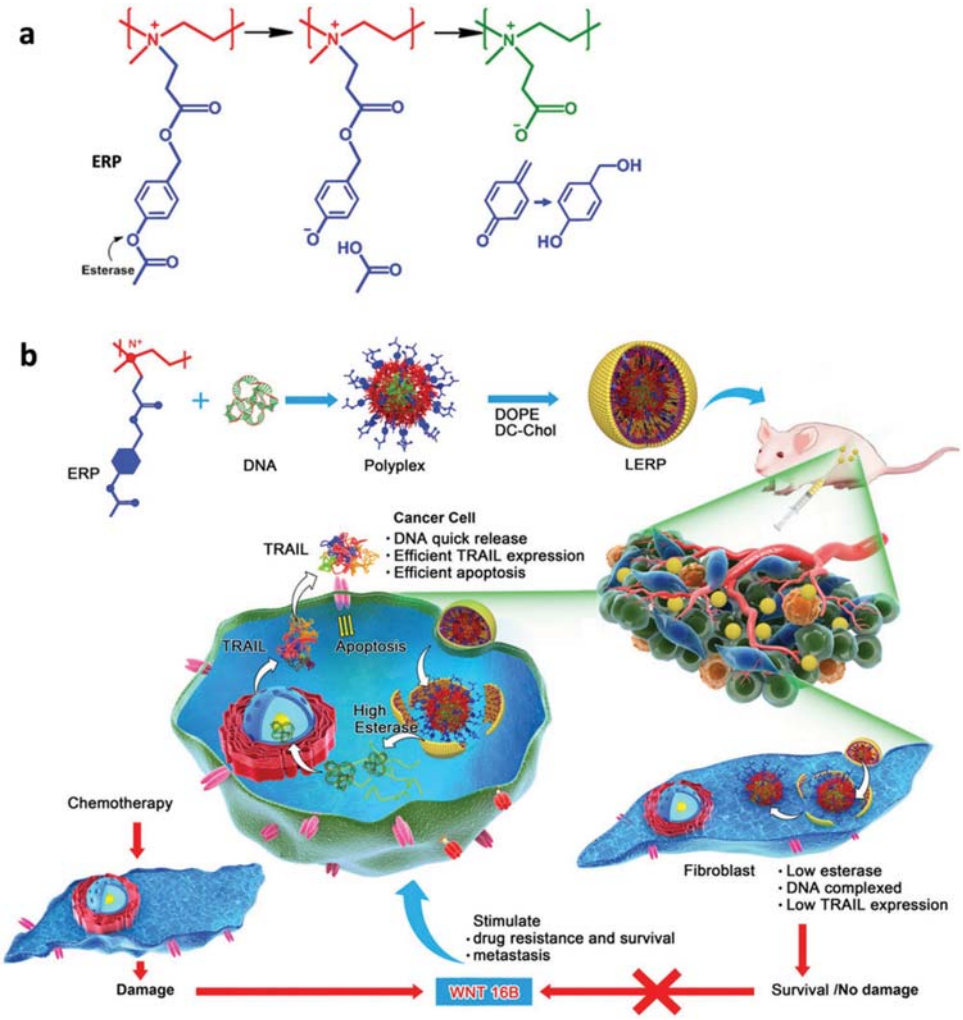

Figure 1. Illustration of a) esterase responsive charge-reversal polymer (ERP) and b) its lipid-coated esterase responsive polyplexes with TRAIL plasmid for i.p. cancer gene therapy. a) The ERP is a PEI whose amines are quaternized with propionic 4-acetoxybenzyl ester. The hydrolysis of the phenolic acetate triggers elimination of p-hydroxymethylphenol and consequent conversion of the cationic polymer into zwitterionic. b) ERP condenses plasmid DNA into the polyplexes, which are easily coated with DC-Chol/DOPE lipids to form lipidic esterase-responsive polyplexes (LERPs). After i.p. injection into nude mice bearing HeLa tumors, tumor cells internalize LERPs into cytosol rich in esterases. The LERPs disassemble and release the polyplexes to allow the esterases to trigger the charge-reversal of ERP and thus release of the plasmids; these free plasmids enter the nucleus for effective gene expression, inducing apoptosis when delivering TRAIL gene. Tumor fibroblasts may also take up LERPs but their low esterase level cannot efficiently induce the charge-reversal process and the TRAIL plasmids cannot be expressed. As a consequence, the fibroblasts are not activated to produce WNT16B as opposed to chemotherapy drugs, which indiscriminately damage and hyperactivate fibroblasts to excrete WNT16B promoting cancer cell survival and metastasis.

using the plasmid expressing luciferase protein (pLUCI) as a reporter gene. Two controls with similar structures, QPEI-BP and QPEI-M, were included for comparison (Figure 2d). ERP polyplexes achieved the highest transfection efficiency in HeLa cells at an N/P ratio of 14, which was three magnitudes higher than those of QPEI-BP and QPEI-M, and two magnitudes higher than that of the corresponding PEI10k polyplexes at their best N/P ratios (Figure 2d and Figure S2B in the Supporting Information). The transfection efficiency of the QPEI-BP polyplexes was very similar to that of QPEI-M (with persistent cationic charges), suggesting that the benzyl esters were not hydrolyzed efficiently. Thus, the strong binding with DNA of quaternary ammonium groups in these controls led to poor transfection.[11g] Furthermore, ERP polyplex-transfected cells expressed the protein very fast; a significant luciferase chemiluminescence was observed in as short as 2 h transfection and reached the maximum level after 6 h. As a comparison, PEI25k polyplexes had significant gene expression only after 6 h because of the slow DNA release (Figure 2e,f). Similar trends were found in HepG2 and SW480 cells, although the transfection efficiencies of ERP polyplexes in the two cell lines were slightly lower (Figure 2d).

An important design feature of ERP is its selective gene expression in cancer cells over fibroblasts by exploiting the low overall esterase activity in fibroblasts. HeLa cells did have much higher intracellular esterase activity than NIH3T3 cells (Figure S3, Supporting Information) as measured with fluorescein diacetate, a cell-permeating esterase substrate that has

DOI: 10.1002/adma.201603095

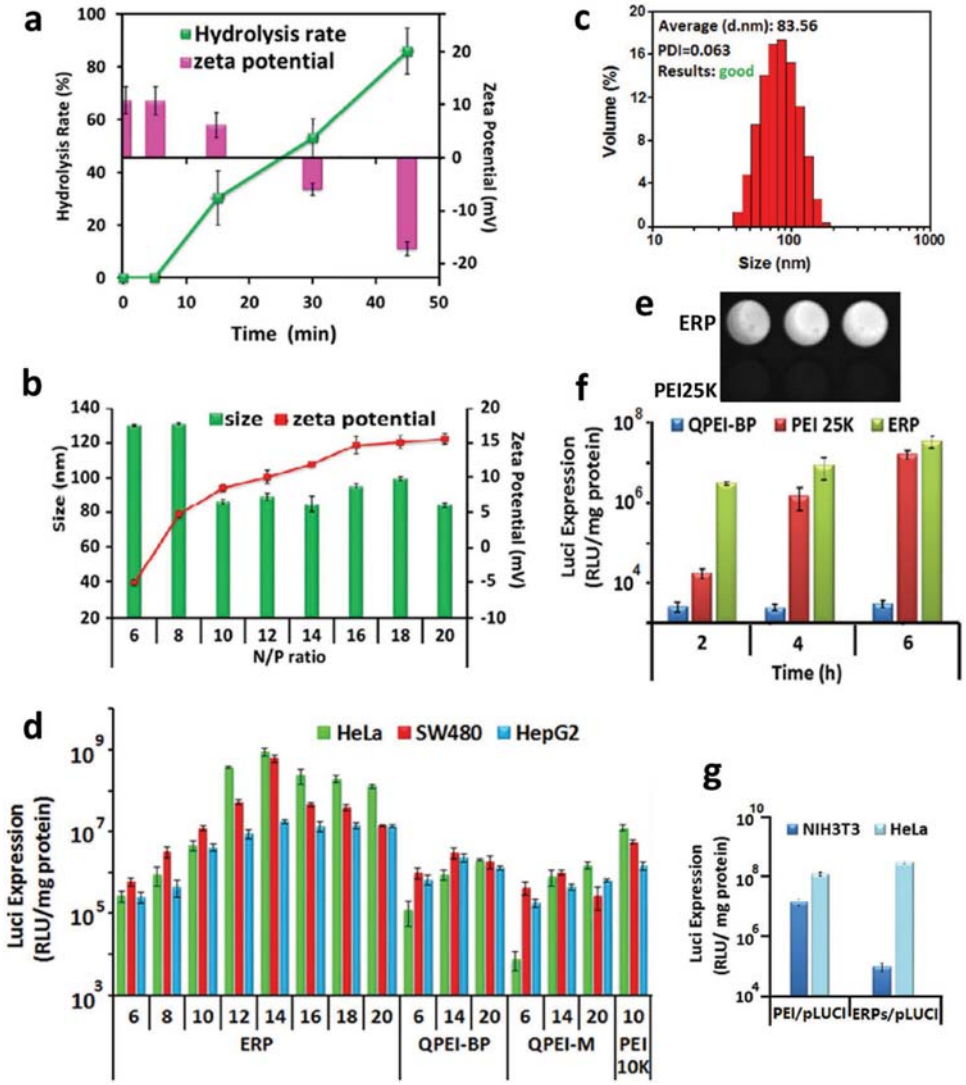

Figure 2. a–c) Hydrolysis and resulting charge-reversal of ERP (a), and its polyplexes (b,c), and d–g) transfection. a) Hydrolysis of the ester groups in ERP as measured by the release of 4-hydroxybenzyl alcohol and the positive-to-negative charge-reversal of ERP once incubated in the esterase solution. Liver esterase, 100 units mL^{-1}; 37 °C; polymer concentration: 5 mg mL^{-1}. b,c) Sizes and corresponding zeta potentials of the ERP/luciferase plasmid DNA (pLUCI) polyplexes formed at different N/P ratios (b), and size distribution of the polyplexes (N/P = 14) measured by dynamic laser scattering (c). d) Luciferase expression of pLUCI polyplexes of ERP and the controls (QPEI-BP, QPEI-M, and PEI) (see Supporting Information, Figure S2B transfection at other N/P ratios) in different cancer cells. 4 h transfection in serum-free medium followed by 44 h incubation in fresh culture medium containing 10% FBS, pLUCI concentration at 2.5 μg mL^{-1}. The luciferase gene expression is expressed as relative luciferase light unit (RLU) per milligram of protein. Error bars represent the s.d. ($n = 3$). e) Chemiluminescence images of the cell lysis of HeLa cells after 2 h incubation with polyplexes (pLUCI, 2.5 μg mL^{-1}). f) Luciferase expression in HeLa cells after 2, 4, or 6 h incubation with polyplexes (luciferase DNA, 2.5 μg mL^{-1}). g) Comparison of luciferase expression in HeLa or NIH3T3 cells of ERP or PEI polyplexes; transfection conditions were same as those in (d). Error bars represent the s.d. ($n = 3$).

been used as a probe to measure esterase activity in cells. The low cytosolic esterase activity in fibroblasts could not efficiently trigger the charge-reversal of ERP and its polyplexes retain the plasmids. As a result, the ERP/pLUCI expression in fibroblasts was 10^3 times lower than that in HeLa cells under the same transfection conditions (Figure 2g). This difference is not caused by the possible cell differences because, as a reference, PEI/pLUCI had similar luciferase expression levels in both cell lines.

The transfection mechanism of ERP polyplexes was studied using confocal microscopy. Cellular internalization of ERP/Cy5-labelled DNA (Cy5-DNA) polyplexes was very fast (**Figure 3**a); in 2 h many red dots were already found inside the cells and their number and intensity increased with culture time. Some of the internalized DNA were associated with green-labelled lysosomes, which appeared as yellow spots, but many DNA dots were not associated with lysosomes (Figure 3b), indicating that the polyplexes were internalized into lysosomes but quickly escaped into the cytosol. To observe the intracellular polyplex dissociation, the polyplexes of Cy5-DNA and FITC-labeled ERP were cultured with cells. In as short as 2 h, most green polymers and red DNA signals were already separated clearly (Figure 3c), indicating that the intracellular polyplexes indeed quickly dissociated. This phenomenon is further confirmed by another important observation that the green signals

ADVANCED MATERIALS
www.advmat.de

Materials Views
www.MaterialsViews.com

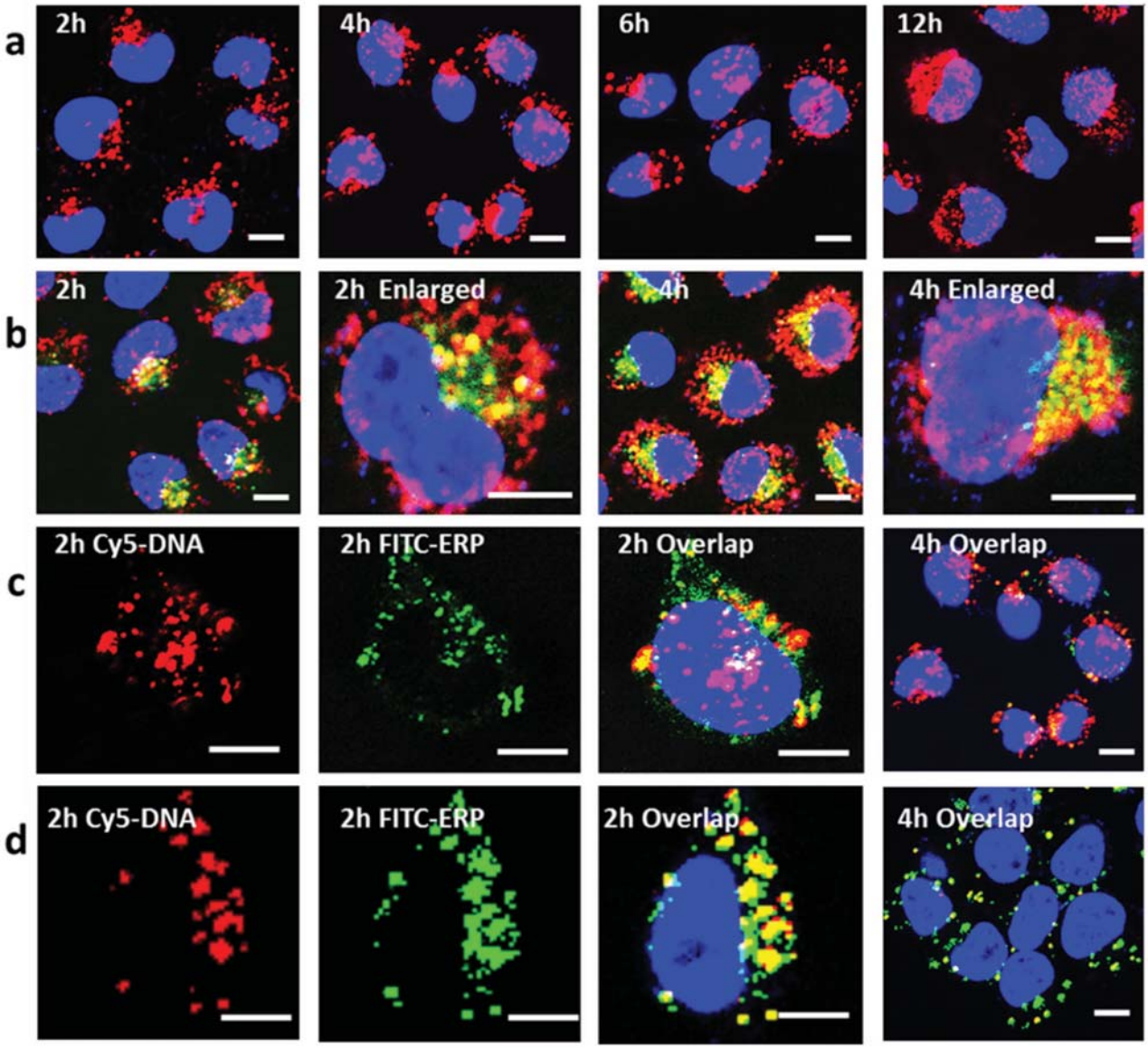

Figure 3. a–d) Intracellular trafficking of ERP/pLUCI polyplexes in HeLa cells (a–c) or in NIH3T3 cells (d) observed by confocal microscopy. a) Cellular uptake by HeLa cells of the polyplexes at different times. DNA was labeled with Cy5 shown in red, and the cell nuclei were stained with Hoechst 33342 shown in blue. b) Lysosomal localization and escape after 2 or 4 h culture; Lysosomes were stained with lysotracker green shown in green; the images are the overlapped ones taken from Cy5-DNA, lysotracker green, and Hoechst 33342 channels. c,d) Polyplex dissociation and free DNA localization in HeLa cells (c) or NIH3T3 cells (d). ERP was labeled with FITC shown in green and Cy5-DNA was shown in red. Luciferase plasmid DNA dose, 0.35 μg mL^{-1}. See the Supporting Information for other images of HeLa cells (Figure S4A, Supporting Information), and cellular uptake and lysosome escape of NIH3T3 cells (Figure S4B, Supporting Information). All scale bars represent 10 μm.

of the polymer molecules were mostly observed in the cytosol and only a little was in the nucleus, while in the nucleus there were many pink dots, i.e., the red (free DNA) signals in blue background. This fast dissociation resulted in fast gene expression in as short as 2 h (Figure 2e,f). Thus, it can be concluded that the fast cellular uptake, lysosomal escape, and dissociation of the ERP polyplexes accounted for the quick and efficient gene expression. In contrast, even though NIH3T3 cells could also quickly took up the polyplexes (Figure S4B, Supporting Information), the intracellular ERP polyplexes could not dissociate (yellow dots, Figure 3d) and almost no free DNA was observed and no DNA was found in the nuclei at the same observed times as HeLa cells (Figure 3c), consistent with the low transfection efficiency (Figure 2g).

To protect polyplexes in vivo from esterase-caused premature dissociation before entering cancer cells, we coated them with a lipid outer layer containing DOPE lipid and cholesteryl 3β-*N*-(dimethylaminoethyl)carbamate (DC-Chol)[17] motivated by the prior work[18] and our recent design of fusogenic lipidic polyplexes.[19] Detailed optimization (Figure S5, Supporting Information) found that the lipid composition at the DOPE/DC-Chol/ERP molar ratio of 30:10:27 produced stable nanoparticles

DOI: 10.1002/adma.201603095

of the ERP polyplexes coated with a stable lipid layer. These lipid-coated, esterase-responsive polyplexes (LERPs) had size and zeta potential of 68 nm in diameter (**Figure 4**a) and +18 mV, respectively. They were stable in solution and even in the presence of esterase and FBS.

Transfection efficiency of LERPs was slightly lower than that of the polyplexes in FBS-free medium, but not very sensitive to serum anymore (Figure 4b). Luciferase expression of LERPs was essentially the same with or without 10% FBS medium. In an extreme case when the transfection was carried out in pure FBS solution (i.e., 100% FBS medium) mimicking blood or ascites, the luciferase expression still remained close to 10^8 RLU mg^{-1} protein level, as opposed to the sharp decrease of PEI and ERP polyplexes (Figure 4b). The cell transfection efficiency of LERPs was observed by the expression of green fluorescent protein (GFP) (Figure S6, Supporting Information) and quantified by flow cytometry in terms of the percentage of GFP-positive cells (Figure S7, Supporting Information) after transfection with EGFP plasmids-loaded LERPs (LERPs/pEGFP). Both experiments indicate that while the presence of FBS sharply decreased the percentage of GFP-positive cells (4.8%) when transfected with PEI/pEGFP polyplexes, FBS surprisingly promoted LERPs/pEGFP to infect cells, where in 100% FBS the GFP-positive cells reached about 65%. These results indicate that the lipid layer did protect ERP from premature hydrolysis by esterase in serum, but once inside cells the ERP polyplexes were able to shed off the lipid layer and exposed to intracellular esterases, as confirmed by confocal microscopy study (Figure S8, Supporting Information). Within 2 h, while there were some yellow dots inside the cells, most lipid (red dots) and ERP (green signals) were already separated.

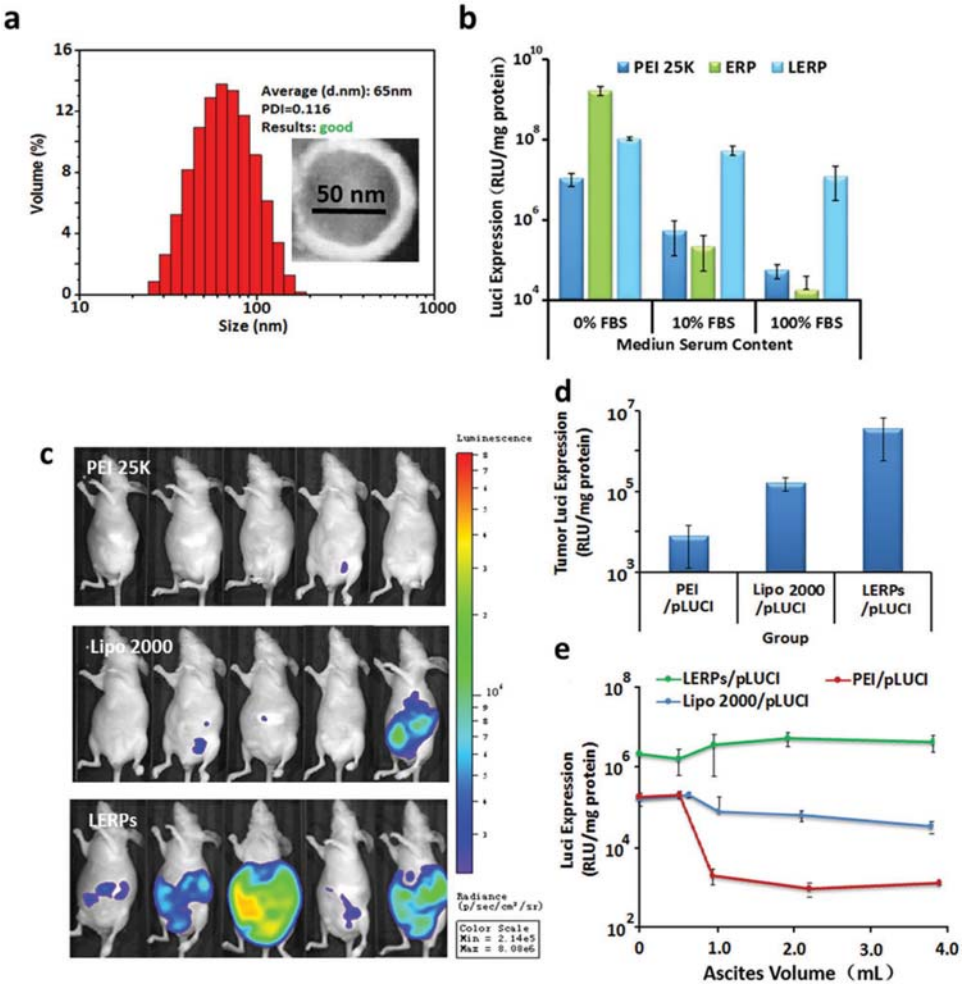

Figure 4. Characterization and in vitro and in vivo gene expression in intraperitoneal (i.p.) HeLa tumors of nude mice of lipid-coated esterase responsive polyplexes (LERPs/pLUCI). a) Size distribution pattern of LERPs/pLUCI determined by DLS; insert, TEM image of an LERP particle; scale bar, 50 nm; N/P = 14; DOPE/DC-Chol/ERP = 30:10:27 (molar). b) Luciferase expression of LERPs/pLUCI compared with ERP and PEI25k polyplexes (DNA, 2.5 μg mL^{-1}) in the absence or presence of serum; 4 h transfection followed by 44 h culture; error bars, s.d. ($n = 3$). c,d) Chemiluminescence imaging (c) and quantitation of HeLa i.p. tumors (d) at 48 h post i.p. injection of the LERPs or PEI25k polyplexes at a pLUCI of 0.5 mg kg^{-1}; error bars, s.d. ($n = 5$). e) Influence of tumor ascites on luciferase expression. Each nude mice was i.p. inoculated with 4×10^6 HeLa cells. After 6, 10, 14, 18, or 22 d postinoculation, mice were i.p. injected with LERPs containing 10 μg luciferase DNA per mouse or the controls, and were sacrificed 2 d after transfection. Ascites were first drawn carefully from each mouse with a syringe, and then the tumors were dissected and lysed for luciferase measurement. Mice with similar ascites volumes were put in one group. Error bars, s.d. ($n = 5$).

ADVANCED MATERIALS
www.advmat.de

www.MaterialsViews.com

In vivo transfection of LERPs was evaluated in HeLa tumors, a mimic of late stage cervical metastatic tumors. Tumor-bearing mice were administered with LERPs/pLUCI or the controls (PBS, positive control Lipo2000/pLUCI and PEI25k/pLUCI) at a dose of 0.5 mg kg^{-1} of pLUCI per i.p. injection. After 48 h, all the mice treated with the LERPs/pLUCI presented strong chemiluminescence, while only one out of the five mice transfected with a commercial transfection reagent Lipo2000 showed chemiluminescence, and those transfected with PEI polyplexes had hardly observable chemiluminescence (Figure 4c). The quantitated luciferase expression in homogenized tumors transfected by LERPs/pLUCI was 450 times higher than that of those transfected by PEI polyplexes, and 20 times higher than those transfected by Lipo2000 (Figure 4d). Very importantly, LERP transfection was not affected by ascites (Figure 4e), which is particularly important in treatment of late-stage i.p. tumors.

The tumor suicide gene TRAIL plasmid DNA (pTRAIL) was loaded into LERPs (LERPs/pTRAIL). LERPs/pTRAIL had very similar size and zeta-potential values to those loaded with luciferase plasmids studied above. The expression of LERPs/pTRAIL in HeLa cells was first assessed by western blot (**Figure 5**a), and was quantified (Figure 5b). Similarly to the results in luciferase and EGFP expression experiments, LERPs/pTRAIL expressed TRAIL more efficiently (three times in 24 h) than PEI/pTRAIL polyplexes and thus induced more efficient apoptosis of the cells (Figure 5c,d), as further verified by flow cytometry (Figure 5e and Figure S9, Supporting Information).

The selectivity of LERP/pTRAIL in inducing apoptosis of HeLa cancer cells to fibroblasts was also tested and compared with three first-line chemotherapy drugs, i.e., irinotecan (CPT11), paclitaxel (PTX), and cisplatin (CDDP) (Figure 5). After transfection with LERPs/pTRAIL for 24 h, LERPs/pTRAIL expressed TRAIL three times more efficiently in HeLa cells than in NIH3T3 (Figure 5a,b). As a consequence, most HeLa cells looked apoptotic but NIH3T3 cells were unaffected (Figure 5c–e and Figure S9, Supporting Information). Flow cytometry analysis indicated that after 24 h LERPs/pTRAIL treatment induced 71% of the HeLa cells apoptotic, most of which were already at late-stage, but did not induce more NIH3T3 cells apoptotic than the PBS control (8.3%). This selective killing of LERPs/pTRAIL was further supported by coculturing other cancer cells with NIH3T3 or their tumors, where the treatment did not affect

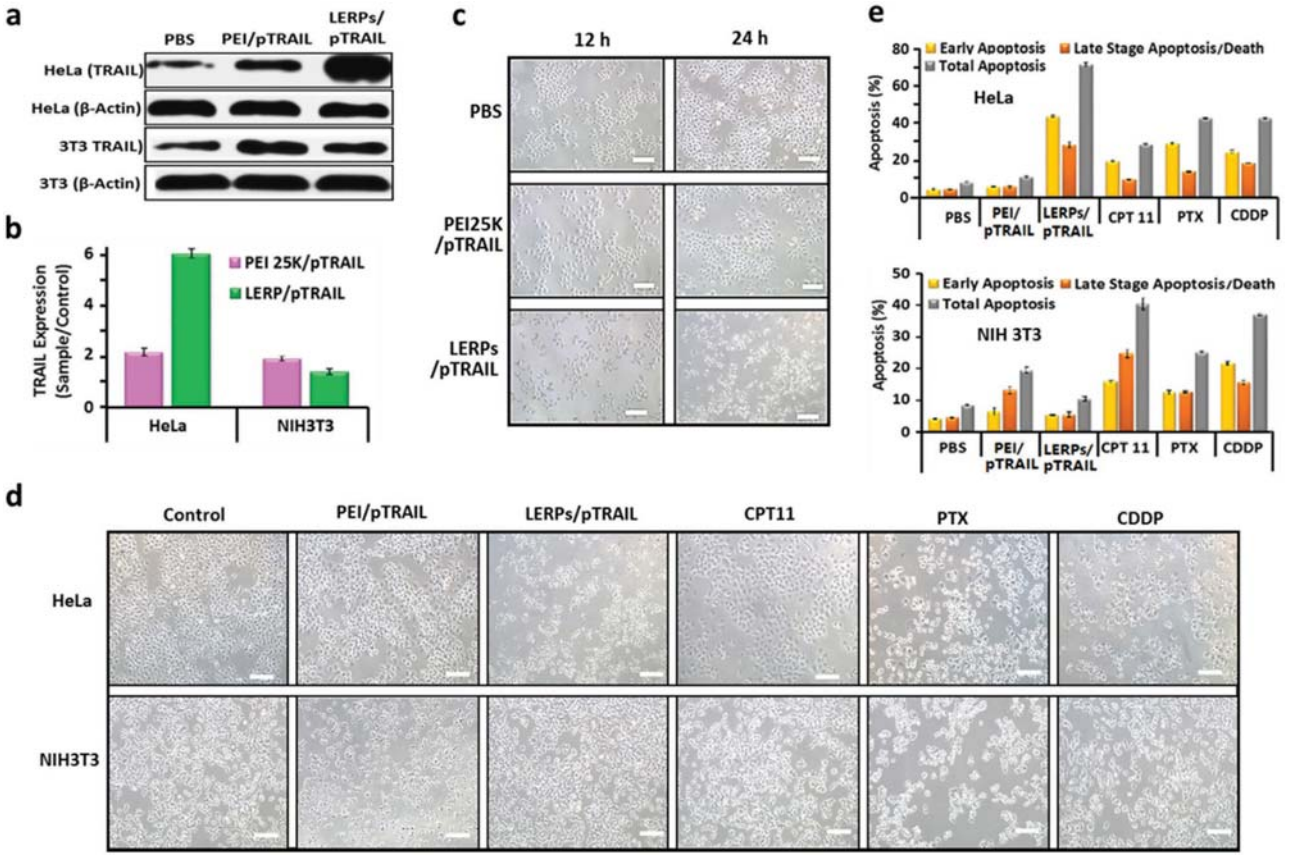

Figure 5. In vitro TRAIL expression induced killing of HeLa cancer cells and NIH3T3 fibroblasts and comparison with chemotherapy drugs. a,b) Western blot (a) and quantitative calculation (b) of TRAIL expression normalized to that of the corresponding PBS control of HeLa cells or NIH3T3 cells. 2×10^5 HeLa or NIH3T3 cells were transfected with PEI polyplexes or LERPs/pTRAIL at 1 μg mL^{-1} of TRAIL plasmid DNA in 10% FBS-containing medium for 4 h and then cultured in fresh culture medium for 20 h. c) Images of cells after being treated with LERPs/pTRAIL or PEI/pTRAIL polyplexes at a DNA dose of 2 μg mL^{-1} for 4 h in 10% FBS-containing medium and then cultured in fresh medium for 8 or 20 h. Scale bar = 100 μm. d,e) Images (d) and the corresponding apoptosis analysis (e) using flow cytometry of HeLa and NIH3T3 cells after transfected for 4 h at a pTRAIL dose of 2 μg mL^{-1} and then cultured in fresh medium for 20 h, compared with the cells incubated with CPT11 (10 μg mL^{-1}), CDDP (5 μg mL^{-1}) or PTX (10 μg mL^{-1}) for 24 h. Scale bar = 100 μm. Error bars represent the s.d. ($n = 3$).

Adv. Mater. **2016**,
DOI: 10.1002/adma.201603095

NIH3T3 cells, but few cancer cells could survive the treatment (Figure S10, Supporting Information). In contrast, PEI/pTRAIL caused 11% of the HeLa cells and 20% of NIH3T3 cells apoptotic even though its TRAIL expressions in both cells were similar (Figure 5b). PTX and CDDP killed both cells efficiently at a similar level (around 40% apoptosis in 24 h), and CPT11 induced even more NIH3T3 cell death than it did in HeLa cells.

In vivo TRAIL expression and induced apoptosis of cancer cells in tumors treated with LERPs/pTRAIL or PEI/pTRAIL were first probed in i.p. tumors. After two LERPs/pTRAIL treatments, the dissected tumors were found heavily expressing TRAIL, as detected by western blots (Figure S11, Supporting Information), and after the fourth treatment extensive cell apoptosis was found, as compared with those treated with PEI/pTRAIL and detected by TUNEL assay (Figure S11, Supporting Information).

The in vivo therapeutic efficacy of LERPs/pTRAIL against i.p. tumors was evaluated using a treatment regime given in **Figure 6**a. The treatment was started on the day 6 post-inoculation and was run on a three-day schedule for four treatments. The first group of mice was sacrificed 3 d after the fourth injection (i.e., day 18). All tumor nodules in the abdominal cavities were dissected and collected (see tumor Dissection 1) to evaluate therapeutic efficacy. The second group of mice received no further treatment and was sacrificed 15 d later for tumor dissection (i.e. day 30, see tumor Dissection 2) to evaluate tumor relapse.

Tumor burdens of the mice after the treatments are shown in Figure 6b,c. Apparently, the carrier LERP/pLUCI, used as a control, had no treatment effect. The average tumor weight per mouse treated with LERPs/pTRAIL, PTX, or cisplatin was similar and all were significantly lower than those of the untreated mice ($P < 0.01$). LERPs/pTRAIL was more effective in tumor suppression than PEI/pTRAIL in terms of both tumor number (2 ± 1 vs 10 ± 6 tumor nodules per mouse) and tumor mass (35 ± 38 mg vs 267 ± 113 mg per mouse) ($P < 0.05$) and

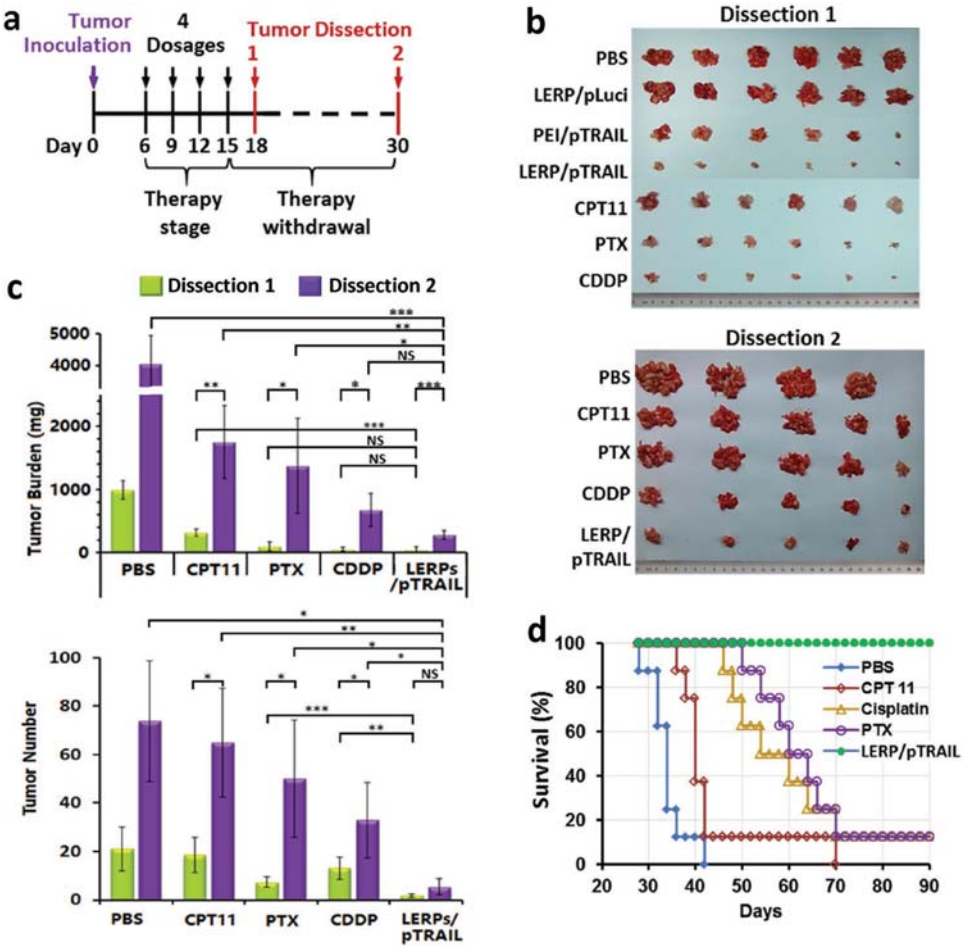

Figure 6. Growth inhibition and regression of HeLa i.p. tumors treated with LERPs/pTRAIL or clinically relevant chemotherapy drugs. a) Treatment regime. 4 ×10^6 HeLa cells were i.p. injected into the peritoneal cavities of nude mice. On day 6 the treatments were initiated by i.p. injection on an every-three-day schedule for four times (pTRAIL DNA dose, 0.5 mg kg^{-1}; CPT11, 10 mg kg^{-1}; PTX, 10 mg kg^{-1}; CDDP, 5 mg kg^{-1}). The mice in each treatment group were then divided into three subgroups. One group of mice was sacrificed three days after the fourth injection and the i.p. tumors were dissected (Dissection 1, $n = 6$); the second group received no further treatment and was sacrificed 15 d after the fourth injection for tumor dissection (Dissection 2, $n = 5$); the third group of mice was maintained without treatment for 90 d. b) Dissected tumor nodules of mice at Dissection 1 and Dissection 2 studies (One mouse in the PBS group died before Dissection 2). c) The average tumor weights and numbers per mouse in each group. (***$P < 0.001$; ** $P < 0.01$; * $P < 0.05$). d) Survival curves of mice receiving different treatments.

ADVANCED MATERIALS
www.advmat.de

Materials Views
www.MaterialsViews.com

also CPT11 (23 ± 7 tumors, 313 ± 35 mg per mouse, $P < 0.01$). Another interesting finding is that mice treated with LERPs/pTRAIL had significantly less number of tumor nodules than those treated by the well-known potent anticancer drugs PTX or cisplatin, even though the average tumor burdens of these groups were similar (Figure 6b,c).

During the 15 d treatment-free period, the mice in the PBS group started to build up ascites from day 22 postinoculation, and one of them died on day 28 due to heavy ascites. On day 30 (Dissection 2), the CPT11-treated group had a much increased tumor burden, by 6 times to 1967 mg per mouse in weight and 3 times to 62 tumor nodules per mouse in number. Accordingly, three in five mice had ascites. Notably, although the four treatments with PTX initially suppressed tumor growth, after 15 d the tumors rebounded (by 14 times to 1733 mg per mouse in weight and by 6 times to 45 tumors per mouse in number). The CDDP-treated group had the smallest increase in tumor burden, by 10 times to 733 mg per mouse in weight and by 3 times to 34 tumors per mouse in number. In summary, the number of tumors in the mice that had received chemotherapy significantly increased during the treatment-free period, indicating the formation of new tumors due to metastasis. Indeed, in these chemotherapy groups many small tumor nodules spread over the intestine and mesentery, and thus ascites were generated in most mice, and several tumors even metastasized to liver and spleen (Figure S12, Supporting Information).

Compared with the severe recurrence during the treatment-free period of the three drug-treated groups, the tumors in the mice that received LERPs/pTRAIL therapy grew larger, from ≈50 to 283 mg per mouse, but the number of tumor nodules per mouse did not significantly increase. Indeed, only few relatively large opaque tumors were found on the mesentery of the LERPs/pTRAIL-treated mice, no tumors were found on their intestine, and no metastatic tumors were found in their liver, spleen and other organs in their peritoneal cavities (Figure S12, Supporting Information). This is a notable difference between the gene therapy group and the chemotherapy-treated groups, indicating that although few tumors survived the four LERPs/pTRAIL treatments, but they grew only slightly and sparsely disseminated new tumors during the therapy withdrawal period.

The prognosis of the LERPs/pTRAIL gene therapy compared with the three drugs is further proven by the long-term survival after the treatments (Figure 6d). The PBS-treated mice quickly built up ascites (as evidenced by the quick increase in body weight, Figure S13, Supporting Information), and then died with a median survival time (ST_{50}) of 34 d. The CPT11- or PTX-treated mice started to build up ascites later with prolonged ST_{50} values, 40 d for the CPT11 group and 60 d for the PTX group, respectively. The CDDP-treated mice did not build up ascites but their body weights decreased significantly during the treatment stage and recovered only slowly after the treatment was stopped (Figure S13, Supporting Information). This group had an ST_{50} of 54 d (Figure 6d) but all mice had poor health condition (Figure S14 and Video S2, Supporting Information). Very significantly, all the mice treated with LERPs/pTRAIL were physiologically sound (Figure S14 and Video S2, Supporting Information) even at the endpoint of the experiment (90 d) (Figure 6d). After the dissection of these mice we found that there were only few opaque tumors in their peritoneal cavities.

The underlying mechanism of the LERPs/pTRAIL gene therapy compared with three drugs was preliminarily investigated (**Figure 7**). The tumors were dissected after the fourth treatment, fixed and sectioned for analysis. H&E staining indicated that tumors treated with LERPs/pTRAIL had reduced cell densities compared to those of the PBS, PEI/pTRAIL, and chemotherapy-treated groups. Caspase-3 immunohistology revealed that in the LERPs/pTRAIL-treated tumors most cells were Caspase 3 positive, indicating cell apoptosis, but tumors in the chemotherapy groups had much less Caspase 3. A very unique phenomenon is that the LERPs/pTRAIL-treated tumors had much fewer cancer cells but much more fibroblast cells than chemotherapy-treated tumors, where tumor cell nests were still very clearly visible (Figure 7a). Fibroblast contents of the tumors were quantified by western blot using α-SMA as the marker (Figure 7b). Clearly, LERPs/pTRAIL-treated tumors had even more fibroblasts than the PBS control tumors, but tumors after chemotherapy had much less fibroblasts present. These results corroborate the results of in vitro experiments (Figure 5) that LERPs/pTRAIL treatment selectively eliminated cancer cells but spared fibroblasts. Importantly, the upregulated α-SMA density after LERPs/pTRAIL treatment could indicate exciting therapeutic outcomes since low intratumoral α-SMA expression was associated with poor prognosis.[20]

Attacking fibroblasts have been shown to induce their hyperactivation of multiple pathways to secrete WNT16B,[10] which subsequently promotes tumor cell survival and metastasis and attenuating cytotoxicity of chemotherapy.[10a] Thus, WNT16B contents of the tumors were quantified by western blot (Figure 7b). Tumors treated with LERPs/pTRAIL contained less WNT16B than the PBS control. PTX-treated tumors also contained fewer fibroblasts, but had an elevated concentration of WNT16B. CDDP-treated tumors contained low level of WNT16B. To realistically compare the WNT16B expression ability of fibroblasts in these tumors, the intensity of WNT16B was normalized to WNT16B/α-SMA value to reflect the WNT16B expression per unit of fibroblasts in tumor (Figure 7c and Figure S15, Supporting Information). Clearly, PTX and CDDP treatments significantly stimulated fibroblasts to express WNT16B by two to three times compared with the PBS group, but LERP/pTRAIL treatment deactivated fibroblasts' WNT16B expression. Thus, LERPs/pTRAIL had two characters, the efficient TRAIL expression in cancer cells inducing potent cancer cell apoptosis and the low TRAIL expression in fibroblasts causing no damage and deactivating them not to express WNT16B, accounting for the least tumor relapse and the lowest number of new tumors, consequently much prolonged survival when compared to chemotherapy (Figure 6).

In addition to its therapeutic advantage, the LERPs/pTRAIL gene therapy did not show any noticeable toxicity or side effects (Figure S16–S18, Supporting Information). The body weight change is a reflection of long-term toxicity of a treatment. The CDDP treatment caused severe weight loss. The mice treated with CPT11 or PTX at the doses used here did not lose weight but quickly built up ascites (Figure S13, Supporting Information). In contrast, the LERPs/pTRAIL therapy caused neither noticeable acute nor long-term toxicities and the mice

Adv. Mater. 2016,
DOI: 10.1002/adma.201603095

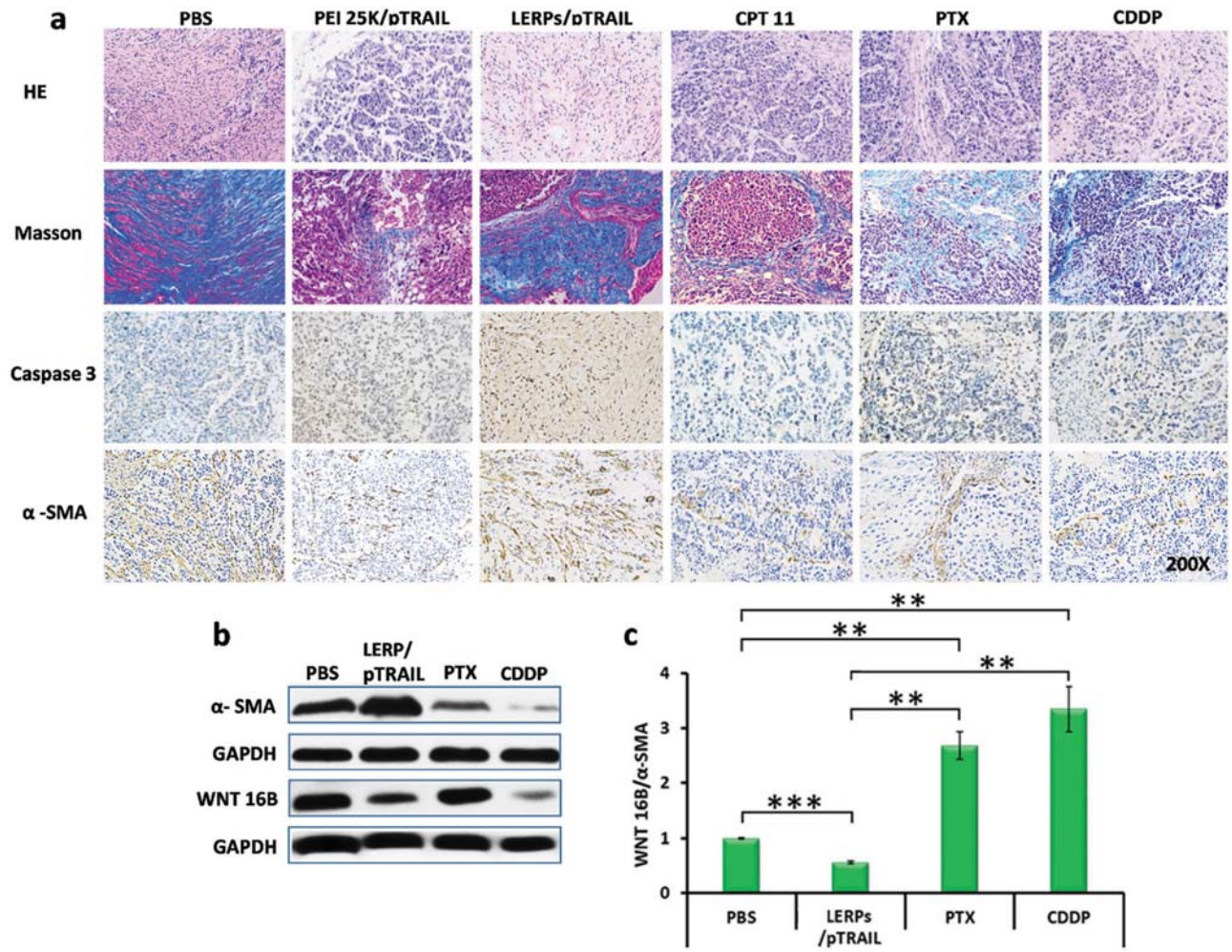

Figure 7. Tumor analysis. a) Histological and immunohistochemical analysis of i.p. HeLa tumors after the 4 treatments. Tissue paraffin sections were 5 µm thick. b) Western blot analysis of expression of α-SMA and WNT16B in the tumors. c) WNT16B content in tumors in terms of per unit of α-SMA. The grey scale of each band in *b* was quantitated using Image J 1.47v software and normalized to the corresponding GADPH intensity (Figure S15, Supporting Information). The value of WNT16B/GADPH divided by that of α-SMA/GADPH produced the corresponding value of WNT16B/SMA.

group grew steadily. The livers of the PTX-treated mice had blood dots and large vacuoles, i.e., hemolytic tissue disruption and CDDP caused severe kidney damage in the form of cracks and spliced fragments as reported (Figure S16, Supporting Information). Both the CPT11 treatment and the PTX treatment also caused splenomegalia (two to three times). In contrast, none of these signs was found in LERP/pTRAIL-treated mice (Figure S17, Supporting Information). The main factors in the whole blood chemistry of the mice were further analyzed (Figure S18, Supporting Information). As expected, the chemotherapy drugs altered many of these factors, but LERP/pTRAIL did not. Together, these results suggest that intraperitoneal administration of the LERP/pTRAIL gene therapy is safer than chemotherapy with PTX, CPT11, or CDDP.

In conclusion, we have designed an esterase-responsive charge-reversal polymer (ERP), whose polyplexes had a selective gene expression in the cancer cells high in esterases, but conserved fibroblasts owing to their low esterase activity. Such polyplexes carrying TRAIL plasmids effectively induced apoptosis of HeLa cells but did not activate fibroblasts to secrete WNT16B, enabling the TRAIL gene therapy to exert potent anticancer activity with few side effects. This overcomes the common problem of chemotherapy drugs, which indiscriminately kill and damage fibroblasts activating them to secrete WNT16B that stimulates the surviving cancer cells to be drug resistant and metastatic. Thus, this work demonstrates a novel approach to selective gene expression in cells via responsive dissociation of polyplexes triggered by intracellular signals.

Supporting Information

Supporting Information is available from the Wiley Online Library or from the author.

Acknowledgements

This work was supported by the National Key Basic Research Program of China (2014CB931900) and the National Natural Science Foundation of China (NSFC 51390481, 51403185 and U1501243). All animal studies

were approved by the Animal Care and Use Committee of Zhejiang University in accordance with the guidelines for the care and use of laboratory animals.

Received: June 12, 2016
Revised: July 31, 2016
Published online:

[1] a) A. B. Hill, M. Chen, C.-K. Chen, B. A. Pfeifer, C. H. Jones, *Trends Biotechnol.* **2016**, *34*, 91; b) M. A. Mintzer, E. E. Simanek, *Chem. Rev.* **2009**, *109*, 259; c) R. Kanasty, J. R. Dorkin, A. Vegas, D. Anderson, *Nat. Mater.* **2013**, *12*, 967; d) J. E. Dahlman, C. Barnes, O. F. Khan, A. Thiriot, S. Jhunjunwala, T. E. Shaw, Y. P. Xing, H. B. Sager, G. Sahay, L. Speciner, A. Bader, R. L. Bogorad, H. Yin, T. Racie, Y. Z. Dong, S. Jiang, D. Seedorf, A. Dave, K. S. Sandhu, M. J. Webber, T. Novobrantseva, V. M. Ruda, A. K. R. Lytton-Jean, C. G. Levins, B. Kalish, D. K. Mudge, M. Perez, L. Abezgauz, P. Dutta, L. Smith, K. Charisse, M. W. Kieran, K. Fitzgerald, M. Nahrendorf, D. Danino, R. M. Tuder, U. H. von Andrian, A. Akinc, D. Panigrahy, A. Schroeder, V. Koteliansky, R. Langer, D. G. Anderson, *Nat. Nanotechnol.* **2014**, *9*, 648.

[2] M. R. Molla, P. A. Levkin, *Adv. Mater.* **2016**, *28*, 1159.

[3] a) M. Goldberg, K. Mahon, D. Anderson, *Adv. Drug Delivery Rev.* **2008**, *60*, 971; b) M. E. Davis, J. E. Zuckerman, C. H. J. Choi, D. Seligson, A. Tolcher, C. A. Alabi, Y. Yen, J. D. Heidel, A. Ribas, *Nature* **2010**, *464*, 1067; c) J. E. Zuckerman, M. E. Davis, *Nat. Rev. Drug Discovery* **2015**, *14*, 843; d) A. Wittrup, J. Lieberman, *Nat. Rev. Genet.* **2015**, *16*, 543; e) K. Zhou, L. H. Nguyen, J. B. Miller, Y. Yan, P. Kos, H. Xiong, L. Li, J. Hao, J. T. Minnig, H. Zhu, D. J. Siegwart, *Proc. Natl. Acad. Sci. USA* **2016**, *113*, 520; f) C. J. Cheng, R. Bahal, I. A. Babar, Z. Pincus, F. Barrera, C. Liu, A. Svoronos, D. T. Braddock, P. M. Glazer, D. M. Engelman, W. M. Saltzman, F. J. Slack, *Nature* **2015**, *518*, 107; g) H. Wang, P. Agarwal, S. Zhao, J. Yu, X. Lu, X. He, *Adv. Mater.* **2016**, *28*, 347.

[4] X. Xu, K. Xie, X.-Q. Zhang, E. M. Pridgen, G. Y. Park, D. S. Cui, J. Shi, J. Wu, P. W. Kantoff, S. J. Lippard, R. Langer, G. C. Walker, O. C. Farokhzad, *Proc. Natl. Acad. Sci. USA* **2013**, *110*, 18638.

[5] a) C. Liu, J. Wen, Y. Meng, K. Zhang, J. Zhu, Y. Ren, X. Qian, X. Yuan, Y. Lu, C. Kang, *Adv. Mater.* **2015**, *27*, 292; b) Y. Dong, K. T. Love, J. R. Dorkin, S. Sirirungruang, Y. Zhang, D. Chen, R. L. Bogorad, H. Yin, Y. Chen, A. J. Vegas, C. A. Alabi, G. Sahay, K. T. Olejnik, W. Wang, A. Schroeder, A. K. R. Lytton-Jean, D. J. Siegwart, A. Akinc, C. Barnes, S. A. Barros, M. Carioto, K. Fitzgerald, J. Hettinger, V. Kumar, T. I. Novobrantseva, J. Qin, W. Querbes, V. Koteliansky, R. Langer, D. G. Anderson, *Proc. Natl. Acad. Sci. USA* **2014**, *111*, 3955.

[6] a) S. T. Crowley, K. G. Rice, *J. Controlled Release* **2015**, *219*, 457; b) U. Laechelt, E. Wagner, *Chem. Rev.* **2015**, *115*, 11043.

[7] a) C. J. Bishop, K. L. Kozielski, J. J. Green, *J. Controlled Release* **2015**, *219*, 488; b) L. Yin, Z. Song, K. H. Kim, N. Zheng, N. P. Gabrielson, J. Cheng, *Adv. Mater.* **2013**, *25*, 3063; c) M. Li, S. Schlesiger, S. K. Knauer, C. Schmuck, *Angew. Chem., Int. Ed.* **2015**, *54*, 2941; d) H. Wang, Y. Wang, Y. Wang, J. Hu, T. Li, H. Liu, Q. Zhang, Y. Cheng, *Angew. Chem., Int. Ed.* **2015**, *54*, 11647; e) B. Zhang, X. P. Ma, M. H. Sui, E. V. Kirk, W. J. Murdoch, M. Radosz, N. M. Lin, Y. Shen, *Chin. J. Polym. Sci.* **2015**, *33*, 908. f) M. Li, M. Ehlers, S. Schlesiger, E. Zellermann, S. K. Knauer, C. Schmuck, *Angew. Chem., Int. Ed.* **2016**, *55*, 598; g) L.-H. Wang, D.-C. Wu, H.-X. Xu, Y.-Z. You, *Angew. Chem., Int. Ed.* **2016**, *55*, 755; h) M. R. Molla, P. A. Levkin, *Adv. Mater.* **2016**, *28*, 1159; i) B. Zhao, Z. Zhou, Y. Shen, *Chin. J. Polym. Sci.* **2016**, *34*, 94.

[8] a) J. Yang, W. Hendricks, G. Liu, J. M. McCaffery, K. W. Kinzler, D. L. Huso, B. Vogelstein, S. Zhou, *Proc. Natl. Acad. Sci. USA* **2013**, *110*, 14717; b) H. Akita, R. Ishiba, R. Togashi, K. Tange, Y. Nakai, H. Hatakeyama, H. Harashima, *J. Controlled Release* **2015**, *200*, 97; c) P. Xu, S. Y. Li, Q. Li, E. A. Van Kirk, J. Ren, W. J. Murdoch, Z. Zhang, Y. Shen, *Angew Chem. Int.* Ed. **2008**, *47*, 1260.

[9] a) J. Shi, J. L. Choi, B. Chou, R. N. Johnson, J. G. Schellinger, S. H. Pun, *ACS Nano* **2013**, *7*, 10612; b) X. Zhou, X. Liu, B. Zhao, X. Liu, D. Zhu, N. Qiu, Q. Zhou, Y. Piao, Z. Zhou, J. Tang, Y. Shen, *J. Controlled Release* **2016**, *234*, 90.

[10] a) Y. Sun, J. Campisi, C. Higano, T. M. Beer, P. Porter, I. Coleman, L. True, P. S. Nelson, *Nat. Med.* **2012**, *18*, 1359; b) A. C. Obenauf, Y. Zou, A. L. Ji, S. Vanharanta, W. Shu, H. Shi, X. Kong, M. C. Bosenberg, T. Wiesner, N. Rosen, R. S. Lo, J. Massagué, *Nature* **2015**, *520*, 368.

[11] a) M. A. Wolfert, P. R. Dash, O. Nazarova, D. Oupicky, L. W. Seymour, S. Smart, J. Strohalm, K. Ulbrich, *Bioconjugate Chem.* **1999**, *10*, 993; b) G. Byk, B. Wetzer, M. Frederic, C. Dubertret, B. Pitard, G. Jaslin, D. Scherman, *J. Med. Chem.* **2000**, *43*, 4377; c) H. Lomas, I. Canton, S. MacNeil, J. Du, S. P. Armes, A. J. Ryan, A. L. Lewis, G. Battaglia, *Adv. Mater.* **2007**, *19*, 4238; d) X. A. Jiang, Y. R. Zheng, H. H. Chen, K. W. Leong, T. H. Wang, H. Q. Mao, *Adv. Mater.* **2010**, *22*, 2556; e) X. X. Zhang, C. A. H. Prata, J. A. Berlin, T. J. McIntosh, P. Barthelemy, M. W. Grinstaff, *Bioconjugate Chem.* **2011**, *22*, 690; f) J. Zhou, J. Liu, C. J. Cheng, T. R. Patel, C. E. Weller, J. M. Piepmeier, Z. Jiang, W. M. Saltzman, *Nat. Mater.* **2012**, *11*, 82; g) S. J. Park, W. Park, K. Na, *Adv. Funct. Mater.* **2015**, *25*, 3472.

[12] a) L. R. Carr, S. Jiang, *Biomaterials* **2010**, *31*, 4186; b) A. Sinclair, T. Bai, L. R. Carr, J. R. Ella-Menye, L. Zhang, S. Jiang, *Biomacromolecules* **2013**, *14*, 1587; c) J. Zhang, Z. Wang, W. Lin, S. Chen, *Biomaterials* **2014**, *35*, 7909.

[13] D. Basavaiah, S. B. Raju, *Synth. Commun.* **1994**, *24*, 467.

[14] L. W. Seymour, Y. Miyamoto, H. Maeda, M. Brereton, J. Strohalm, K. Ulbrich, R. Duncan, *Eur. J. Cancer* **1995**, *31A*, 766.

[15] Z. Zhang, G. Cheng, L. R. Carr, H. Vaisocherová, S. Chen, S. Jiang, *Biomaterials* **2008**, *29*, 4719.

[16] C. A. H. Prata, Y. Zhao, P. Barthelemy, Y. Li, D. Luo, T. J. McIntosh, S. J. Lee, M. W. Grinstaff, *J. Am. Chem. Soc.* **2004**, *126*, 12196.

[17] X. Cheng, R. J. Lee, *Adv. Drug Delivery Rev.* **2016**, *99*, 129.

[18] a) T. Nakamura, H. Akita, Y. Yamada, H. Hatakeyama, H. Harashima, *Acc. Chem. Res.* **2012**, *45*, 1113; b) M. Hyodo, Y. Sakurai, H. Akita, H. Harashima, *J. Controlled Release* **2014**, *193*, 316.

[19] X. Liu, J. Xiang, D. Zhu, L. Jiang, Z. Zhou, J. Tang, X. Liu, Y. Huang, Y. Shen, *Adv. Mater.* **2016**, *28*, 1743.

[20] a) W. Q. Wang, L. Liu, H. X. Xu, G. P. Luo, T. Chen, C. T. Wu, Y. F. Xu, J. Xu, C. Liu, B. Zhang, J. Long, Z. Y. Tang, X. J. Yu, *Plos One* **2013**, *8*, e71189; b) B. C. Ozdemir, T. Pentcheva-Hoang, J. L. Carstens, X. F. Zheng, C. C. Wu, T. R. Simpson, H. Laklai, H. Sugimoto, C. Kahlert, S. V. Novitskiy, A. De Jesus-Acosta, P. Sharma, P. Heidari, U. Mahmood, L. Chin, H. L. Moses, V. M. Weaver, A. Maitra, J. P. Allison, V. S. LeBleu, R. Kalluri, *Cancer Cell* **2014**, *25*, 719.